Cellulose (2024) 31:6091–6104
https://doi.org/10.1007/s10570-024-05965-y

ORIGINAL RESEARCH

Low temperature effects on the rheological properties of aqueous cellulose nanofiber suspensions

Kiera Thompson Towell · Emily Asenath-Smith

Received: 23 February 2024 / Accepted: 18 May 2024 / Published online: 30 May 2024

Abstract Cellulose nanofibers (CNFs) are a versatile natural material which are currently in use as a reinforcing agent in composite materials. Cellulose composites have a diverse range of applications because of their high strength to weight properties. Neat CNFs readily disperse in water to form a viscous slurry-like suspension making them an easy material to incorporate into composites; however, CNF suspensions have complex rheological properties, and it is vital to understand these properties to optimize their use. Suspensions of CNFs are structured fluids with unique rheological properties. Most notably, they can form stable networked gels at higher concentrations, resisting flow. While there are robust studies of CNF suspensions at ambient and above temperatures, there is little data on the behavior of aqueous CNF suspensions down to 0 ºC. Rheological studies were performed on aqueous CNF suspensions of variable concentrations to map their flow properties below ambient temperatures. The CNF suspensions were made by diluting neat CNF stock without any chemical modifications (e.g., oxidation, base dissolution). At 0.5 wt%, CNF suspensions displayed gel-like properties, but only the 1 wt% CNF suspensions did not flow upon tilting. The viscosity of the CNF suspensions showed an inverse relationship to temperature down to 2 °C regardless of concentration. The yield strength of higher wt% CNF gels demonstrated a similar trend, increasing with both increasing cellulose concentration and decreasing temperature. Cellulose suspensions were confirmed to be shear thinning at low temperatures and demonstrated tunable gel strength and viscosity, which can be utilized for a variety of applications where processing at low temperatures is important.

Keywords Cellulose · Rheology · Nanofibers · Yield stress fluid · Gel-like behavior

K. Thompson Towell · E. Asenath-Smith (✉)
US Army Engineer Research and Development Center (ERDC), Cold Regions Research and Engineering Laboratory (CRREL), 72 Lyme Road, 03755 Hanover, NH, USA
e-mail: Emily.Asenath-Smith@usace.army.mil

Introduction

Cellulose (or cellulosic) materials are naturally derived from plant matter, and therefore support sustainable chemistry and material synthesis goals (Li et al. 2021). They have been used to increase strength and decrease weight of composite materials across a variety of applications, from bio composites to cements (Guan et al. 2020; Bledzki and Gassan 1999; Ardanuy et al. 2015; Sharma et al. 2019; Huber et al. 2012; Hubbe et al. 2008; Zambrano et al. 2020). The beneficial thermal properties of cellulose have also resulted in its use as an aerogel for insulating purposes as well as energy storage (Sen et al. 2022; Liu et al. 2021). In addition to its beneficial properties in solid form, the time and rate dependent

gel-like properties of nanocellulose make it an adaptable liquid component for polymer extrusion printing and bioinks (Yasim-Anuar et al. 2020; Heggset et al. 2019; Baniasadi et al. 2022). The mechanical and chemical properties, as well as the rheological behavior of nanocellulose, have led to its use in various food applications (Velásquez-Cock et al. 2019; Shi et al. 2014; Zhu et al. 2021). Nanocellulose comes in many different forms, most commonly as CNFs, cellulose nanocrystals (CNCs), and bacterial nanocellulose (BNC), and can be modified through chemical and enzymatic treatments to enhance the reactivity and change the physiochemical properties (Das et al. 2022; Hubbe et al. 2008; Habibi et al. 2010). Some chemical treatments, like TEMPO oxidation and carboxymethylation, can disintegrate the fibers and dissolve them to produce a transparent hydrogel. The various forms of cellulose all have different aspect ratios, solubility, and rheological properties (Seddiqi et al. 2021). It is vital to understand the rheological properties of neat untreated CNF suspensions to simplify processing, reduce cost, and expand their use in different matrix materials.

The rheology of CNF suspensions is highly dependent on fiber length, aspect ratio, surface chemistry and charge, ionic strength, pH, and cellulose concentration for both steady flow and gel-like properties (Geng et al. 2018; Fall et al. 2011). The dynamic moduli, shear stress, and viscosity all increase as a function of CNF concentration (Pääkkö et al. 2007; Li et al. 2015; Naderi 2017; Wu et al. 2014). Cellulose suspensions demonstrate shear thinning and thixotropic behavior during flow, meaning the viscosity decreases with both applied shear rate and time (Jiang et al. 2021; Iotti et al. 2011). Cellulose is also a structured fluid that demonstrates gel-like behavior, thus for higher concentrations it requires an applied stress to initiate flow (Jiang et al. 2021). Different forms of cellulose have been reported to align with the shear flow in the rheometer and during extrusion processes, decreasing the viscosity of the suspension (Hausmann et al. 2018). At high shear rates, the structure breaks down and no longer displays shear thinning behavior (Iotti et al. 2011; Nechyporchuk et al. 2016).

To support various applications, research has been conducted on the rheology of different cellulose gels and suspensions but none of the studies have considered their behavior at temperatures below ambient (Li et al. 2015; Nechyporchuk et al. 2016; Navard et al. 2012; Pääkkö et al. 2007; Naderi 2017). As temperature increases, the viscosity of cellulose suspensions decreases (Herrick et al. 1983; Navard et al. 2012), while the storage modulus was reported to increase (Lowys et al. 2001; Pääkkö et al. 2007). However, these studies were conducted at temperature ranges at and above room temperature, and do not examine the properties of cellulose suspensions below ambient temperatures. CNF aerogels are made through ice templating and sublimation (Martoïa et al. 2016; Gupta et al. 2018; Flauder et al. 2013; Erlandsson et al. 2018). Therefore, the rheological behavior of cellulose suspensions at temperatures approaching freezing is necessary to control the aerogel structure. It is essential to examine suspensions across a range of temperatures to ensure that the rheological behavior of the CNF suspensions can be understood and controlled for a variety of applications, including production, transport, and storage at colder temperatures.

The CNF suspensions used in this study were mechanically fibrillated aqueous slurries derived from wood pulp with fiber widths of 50 nm and lengths up to several hundred microns (Nanocellulose Data Sheets, UMaine). The aqueous slurries were bleached to remove other compounds including resins, fatty acids, and other extractives (PDC Services, UMaine); however, these slurries were not chemically oxidized or hydrolyzed, and the resulting cellulose nanofiber suspensions are white, opaque, pasty, gel-like dispersions of CNFs, which are highly subject to entanglement.

Herein we report on the rheological properties of aqueous CNF suspensions that were made from mechanically fibrillated slurries and examined at low temperatures while varying the concentration and temperature. The viscosity, shear thinning behavior, storage modulus, and yield stress were monitored as the temperature was varied from room temperature down to 2 °C. The temperature dependence of aqueous cellulose suspensions demonstrates that the rheology of these suspensions can be tuned for various applications by controlling the temperature.

Experimental methods

Materials and equipment

Cellulose nanofibers (CNFs) were sourced from a bulk suspension of 3 wt% solids (Process Development Center, The University of Maine, USA). The

fibers are mechanically fibrillated aqueous slurries derived from wood pulp and were not chemically oxidized or hydrolyzed. The CNFs had a nominal fiber width of 50 nanometers (nm), lengths up to several hundred micrometers (μm), pH = 6, and a surface area of 31–33 m^2/g (measured by nitrogen adsorption using the BET method) (Nanocellulose Data Sheets, UMaine). The CNFs were imaged using atomic force microscopy (AFM) in tapping mode (Dimension Icon, Bruker, USA) (Fig. 1). Dilutions of the CNF solutions were made with deionized water (18.2 MΩ-cm) from a Milli-Q water purification system (Milli-Q model IQ 7000, MilliporeSigma, USA).

A rheometer (HAAKE MARS 60, Thermo Fisher, USA) equipped with a vane rotor and serrated cup were used to conduct the experiments. The Rheowin 4.87 software was used to run the experiments and temperature was controlled with a universal Peltier temperature module with insulated sample hood for a temperature range from − 40 °C to 200 °C.

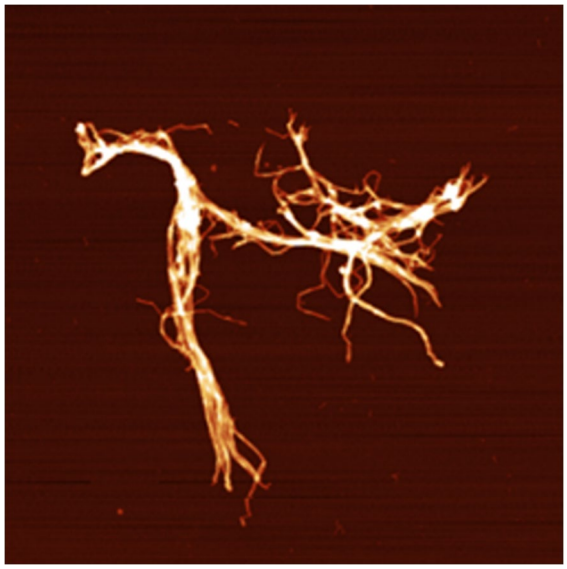

Fig. 1 Atomic force microscopy scan (4 × 4 μm) of cellulose nanofibers showing high aspect ratio and significant presence of entanglements

Methods

Sample preparation

Cellulose nanofiber suspensions were diluted with deionized water from a 3 wt% stock mixture to form 0.1 wt%, 0.5 wt% and 1 wt% CNF suspensions (Fig. 2). While all three CNF suspensions displayed gel-like properties, only the 1 wt% CNF mixture could resist flow upon tipping (Malkin et al. 2023; Flory 1974). These suspensions, as well as pure water, were cooled in a refrigerator at 4 °C prior to testing. For samples that were to be tested at or close to room temperature, the suspensions were stored at room temperature.

Rheological symbols

Rotational measurements

The steady shear flow properties of the cellulose suspensions were measured using rotational

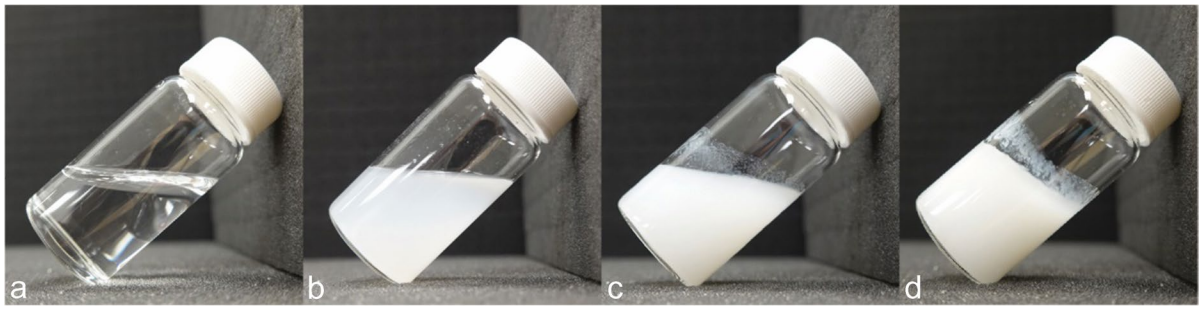

Fig. 2 Pure water (**a**) and suspensions of 0.1 wt% CNFs (**b**), 0.5 wt% CNFs (**c**), and 1 wt% CNFs (**d**). Only the 1 wt% suspension (d) resisted flow upon tipping, classifying it as a gel

experiments with a cup and rotor geometry. A serrated cup was used with a vane rotor, similar to methodology used on mechanically refined CNF suspensions (O'Banion and Shams Es-haghi 2023), to reduce wall slip during the experiments (Nechyporchuk et al. 2015). A pre-shear of 10 s^{-1} was applied for 10 s, followed by a 10 min rest, to ensure a similar starting structure for the CNF samples. Shear rate sweeps were conducted from 0.01 to 100 s^{-1} to encompass a broad range of material properties and behavior during the shear ramp. Data acquisition was started 10 s after rotation was initiated.

The shear rate ramp was used to examine the viscosity and shear stress response of the material during an increase in shear rate. The viscosity and shear stress curves were examined from $\dot{\gamma} = 0.1 - 10\ s^{-1}$ to exclude viscosity plateaus at high and low shear rates, as well as any artifacts from the rheometer (Table 1).

The viscosity of each suspension was extracted from the data at the point where the strain rate was 1 s^{-1}, to compare the relative viscosity of each CNF suspension to the cellulose concentration of the suspension.

Data analysis

The viscosity behavior of the suspensions was fit from the strain rate range of 0.1 to 10 s^{-1} using a power law equation to compare shear thinning behavior (Eq. 1).

Table 1 Rheological symbols, terms, and units used in this work

Symbol	Definition	Units
η	Viscosity	$Pa \bullet s$
γ	Shear Strain	% or unitless
$\dot{\gamma}$	Shear Strain Rate	s^{-1}
n	Shear Thinning Constant	unitless
τ	Shear Stress	Pa
τ_y	Shear Stress at Yield	Pa
f	Frequency	Hz
$G\prime$	Storage Modulus	Pa
$G\prime\prime$	Loss Modulus	Pa

$$\eta = K\dot{\gamma}^{-n} \tag{1}$$

where η is the viscosity in Pa·s, K is a calculated constant in Pa·s^n, $\dot{\gamma}$ is the shear rate, and n is a shear thinning constant. The suspension displays shear thinning behavior if the constant n is positive, and as n approaches 1 the suspension is more shear thinning.

The shear rate ramp was used to provide a fit for yield stress fluids using the Herschel-Bulkley equation for non-Newtonian fluids to examine the reaction of the shear stress with applied shear strain rate (Eq. 2).

$$\tau = \tau_0 + K\dot{\gamma}^n \tag{2}$$

The Herschel-Bulkley equation is a more complex form of a power law fit to describe the shear stress response, where τ_0 is yield stress, K is the consistency index, and n is the flow index. The suspension is a yield stress fluid if τ_0 is positive, and shear thinning if $n < 1$. The fit was applied over the same range as the power law fit, from $\dot{\gamma} = 0.1 - 10s^{-1}$, to ensure it is a continuous function of strain rate and not affected by high and low strain rates and instrument torque. These equations, and similar versions of them, are commonly used to describe the rheological behaviors of cellulose suspensions (Koponen 2020). The shear thinning behavior was described using a power law fit of the viscosity curves, while the Herschel-Bulkley fit was used to predict yield stresses from the shear stress curves.

Oscillatory measurements

The viscoelastic behaviors of the CNF suspensions were determined using oscillatory strain, frequency, and stress sweeps. The oscillatory measurements were carried out using the same cup and rotor as the rotational measurements because of the low viscosity of some samples.

First, an oscillatory strain sweep was used to find the linear viscoelastic range (LVR), in which the viscoelastic properties are independent of the applied strain. The strain sweep was conducted from 1E-4 to 1 at a frequency of 1 Hz, and the range in which the storage (G') and loss (G") moduli are linear was calculated. The CNF suspensions were then subject to frequency sweeps at a constant strain within the

LVR, chosen to be a strain of 10^{-3}. The frequency was ramped from 0.1 to 100 Hz for the 1 wt% CNF suspensions, and from 0.01 to 10 Hz for the 0 to 0.5 wt% CNF suspensions, to provide the best measurement range for monitoring the gel-like response at 1 Hz. Finally, oscillatory stress sweeps were conducted on the CNF suspensions from 0.001 to 100 Pa, as another method to measure the yield stress of the suspensions. From an oscillatory yield stress sweep, the yield stress can be determined by finding the point where the slope of the strain or storage modulus change with applied stress.

Temperature of measurements

To determine the rheological properties of CNF suspensions at low temperatures, two different methods were applied. Initially, the rheological tests were all conducted at 2 °C for each CNF suspension. For each rotational and oscillatory measurement, 0.1, 0.5 and 1 wt% CNF suspensions were prepared, stored at 4 °C, and then tested at 2 °C in replicates of 3. With the cup and rotor geometry, 28 mL of CNF suspension was used for each experiment. After the tests were conducted for every sample at 2 °C, more 1 wt% CNF suspensions were prepared for rheological experiments at 5, 10, 15, 20, and 25 °C to measure the behavior of the suspension with temperature. For these experiments, the 5 and 10 °C suspensions were stored at 4 °C prior to testing, and the 15, 20, and 25 °C suspensions were stored at room temperature. The sample was allowed to rest for 10 min at the test temperature to equilibrate. The 1 wt% CNF suspensions were tested using a rotational shear rate sweep from 0.001 to 100 s^{-1} and an oscillatory frequency sweep.

Results

The rheological properties of the CNF suspensions were measured using both steady flow rotational measurements, as well as oscillatory measurements to evaluate the gel-like properties of the cellulose suspensions. These experiments provided an overview of the viscosity, yield stress, and gel-like behavior of the CNF suspensions as both the composition and the temperature were changed.

Strain rate sweeps

Shear thinning behavior of the CNF suspensions was measured from strain rate dependent viscosity. For all CNF suspensions the viscosity decreased with applied shear rate and increased with CNF concentration (Fig. 3a).

At low shear rates (below 0.1 s^{-1}) the viscosity began to plateau and was almost constant with shear rate, representing the zero-shear viscosity. In the shear rate range of 0.1–10 s^{-1} the viscosity decreased with a power law relationship to shear rate. The decrease in viscosity for all concentrations of CNFs indicated that the CNF suspensions were shear thinning from strain rates of 0.1 to 10 s^{-1}. At higher shear rates (above 10 s^{-1}) the viscosity plateaued again as it approached its infinite shear viscosity. In this shear

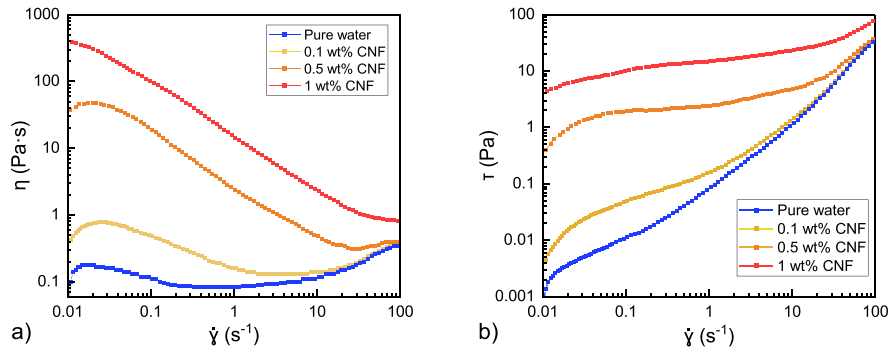

Fig. 3 Viscosity (**a**) and shear stress (**b**) as a function of shear strain rate for different concentration of CNF suspensions. The viscosity of the suspensions decreased with increasing shear rate. The shear stress increased with increasing shear rate and with cellulose concentration. These plots are representative of the trend seen across 3–5 replicates for each concentration

rate range, secondary flows were generated as an artifact of the cup and rotor geometry, causing some flocculation in the fiber networks (Karppinen et al. 2012). The structure, and subsequent breakup, of the flocs contributed to the shear thinning behavior of the CNF solutions, as is consistent in other studies. Over the entire range of the test (0.01 to 100 s^{-1}), the pure water samples did not remain constant with applied shear strain, despite that water is a Newtonian fluid. This is an artifact of the test geometry, conditions, measurement time delay, and high and low rotor speeds, which cause flow and measurement inconsistencies in the high and low shear regimes. In the shear rate range of 0.1 to 10 s^{-1} the viscosity of water is almost constant, and in this regime the properties of the various CNF solutions are examined and compared relative to our measurements of pure water.

The shear stress response of the suspensions during steady flow is shown in Fig. 3b. The shear stress increased with strain rate across the range tested for all samples. In the different regimes of flow the shear stress increased at different rates, with all suspensions experiencing a higher increase in stress below 0.1 s^{-1} and above 10 s^{-1} than they did between 0.1 and 10 s^{-1}. In all regimes, the shear stress at a given shear rate increased with increasing cellulose concentration.

In Table 2 the rheological behavior in the regime between a strain rate of 0.1 s^{-1} and 10 s^{-1} was examined, where the suspensions viscosity and shear stress followed power law and Herschel-Bulkley behavior respectively.

The steady flow experiments were used to compare the viscosity of the CNF suspensions at a strain rate of 1 s^{-1}, and the experimental values are shown in Table 2. The measured viscosity increased with concentration of cellulose. The viscosity of pure water is less than that of the cellulose suspensions, even at concentrations as low at 0.1 wt% cellulose. The commonly reported value for the dynamic viscosity of water at 2 °C is on the scale of 1 mPas, so the viscosity value for 0 wt% CNFs in Table 2 varies significantly. This difference is a result of the test configuration and conditions being optimized for the more viscous CNF solutions, and the error arises due to the low viscosity of water.

Table 2 Viscosity, shear thinning behavior, and calculated yield stress of cellulose suspensions in the range of shear strain rates 0.1–10 s^{-1}

CNF Concentration (wt%)	Viscosity* (Pa·s)	Shear Thinning Exponent *n*	Calculated Yield Stress (Pa)
0	0.084 +/- 0.001	0 +/- 0.01	0.005 +/- 0.005
0.1	0.157 +/- 0.005	0.38 +/- 0.03	0.016 +/- 0.005
0.5	2.8 +/- 0.4	0.90 +/- 0.01	2.2 +/- 0.3
1	14.3 +/- 0.1	0.94 +/- 0.02	11 +/- 1

* The viscosity of the suspensions was measured at a strain rate of 1 s^{-1}

The shear thinning behavior of the CNF suspensions was evaluated by fitting the viscosity curves with a power law equation (Eq. 1)(Quennouz et al. 2016), in the regime between a strain rate of 0.1 s^{-1} and 10 s^{-1}. The shear thinning exponent for the CNF suspensions increased with CNF concentration (Table 2). A suspension is shear thinning if n is less than one, if n is zero the suspension is not shear thinning. A sample of pure water was included to demonstrate that pure water does not display any shear thinning behavior.

The dynamic yield stress of the CNF suspensions was calculated by fitting the shear stress curve with the Herschel-Bulkley equation (Eq. 2) in the aforementioned regime of the shear strain rate testing (O'Banion and Shams Es-haghi 2023). The calculated yield stress of the suspensions increased with increasing cellulose concentration (Table 2), matching the trends observed in the viscosity measurements and shear thinning behavior.

Oscillatory sweeps

Oscillatory sweeps were conducted to examine the gel-like properties of the CNF suspensions in the linear viscoelastic range (LVR) of the suspensions. The pure water samples were not tested using oscillatory sweeps as water does not demonstrate gel-like properties. The LVR was determined by observing the storage (G') and loss (G") moduli of the suspensions during oscillatory strain sweeps in Fig. 4a. Oscillatory frequency sweeps were then conducted on all cellulose suspensions to examine the dependence of the storage moduli on frequency and concentration (Fig. 4b).

The storage and loss moduli of all CNF suspensions were constant and independent of strain up to strain range of 0.001 to 0.01, indicating that the LVR

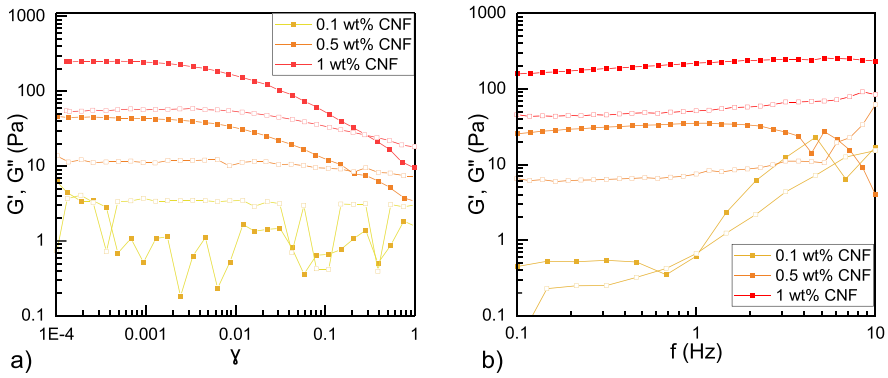

Fig. 4 Storage (filled symbols) and loss (open symbols) moduli for CNF suspensions from oscillatory strain sweeps (**a**) and frequency sweeps (**b**). These plots are representative of the trends seen across 3–5 replicates for each concentration

for the cellulose suspensions goes up to a strain of 0.01. A strain of 10^{-3} was selected for all additional oscillatory sweeps because it was safely in the LVR for all three cellulose suspensions. The 1 wt% cellulose suspension demonstrated moduli dependence on shear at a lower applied shear than the 0.5 wt% cellulose suspensions. The 0.5 and 1 wt% suspensions experienced a decrease in storage and loss moduli at strains above the LVR, but the 0.1 wt% suspension did not show strain dependence and did not show gel-like behavior. The 0.5 and 1 wt% cellulose suspensions clearly had higher storage moduli than loss moduli, demonstrating that they have characteristics similar to a networked gel.

At a constant strain of 10^{-3}, as the frequency of the oscillations was ramped from 0.1 to 10 Hz, the moduli of the 0.5 and 1 wt% CNF suspensions showed only a slight increase with frequency and behaved almost frequency independent until they approached 10 Hz (Fig. 4b). Both the storage and loss moduli increased from the 0.1 wt% CNF suspension to the 1 wt% CNF suspension, indicating the formation of a stronger gel-like network.

Oscillatory stress sweeps were conducted on the 0.5 and 1 wt% CNF suspensions in the LVR as another method to analyze the yield stress of the suspensions (Fig. 5). The 0.1 wt% CNF sample was omitted because it did not have a yield stress.

As the applied stress increases, the slope of the storage modulus and strain changed at a critical applied stress where the suspension began to experience structural breakdown, which was calculated as the yield stress. A clear change in slope of the storage modulus (Fig. 5a) was noted for the 0.5 wt% CNF and 1 wt% CNF samples, with a slight change in slope of the strain curve at the same stress (Fig. 5b).

The storage modulus and yield stress of the cellulose suspensions in the LVR are shown with cellulose concentration in Table 3.

The storage modulus was extracted from the oscillatory frequency sweeps at 1 Hz to compare with cellulose concentration. There was a clear increasing trend between storage modulus and cellulose concentration. The yield stress calculated from the oscillatory stress sweep also showed an increase with cellulose concentration, with structural breakdown

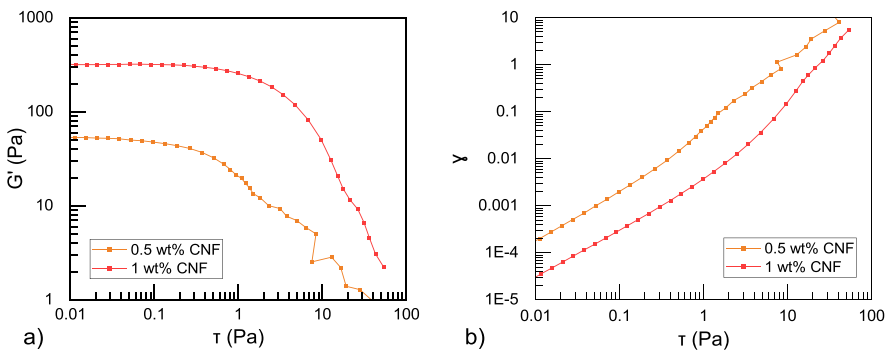

Fig. 5 Oscillation stress sweep for yield stress determination. The storage moduli (**a**) and shear strain (**b**) are plotted against applied shear stress. The yield stress occurred at the point where the slope of the moduli and strain curves changed. These plots are representative of trends from 3–5 replicates for each concentration

Table 3 Storage modulus of cellulose suspensions at 1 Hz and calculated yield stress

Cellulose Concentration (wt%)	Storage Modulus (Pa)	Calculated Yield Stress (Pa)
0.1	0.9 +/- 0.2	N/A
0.5	40 +/- 3	0.04 +/- 0.02
1	305 +/- 100	1.26 +/- 0.09

occurring at a much lower applied stress for the 0.5 wt% CNF suspension than the 1 wt% suspension.

Temperature dependence

Shear rate ramps were conducted at temperatures ranging from 2 ℃ to 25 ℃ to measure the shear response of 1 wt% CNF suspensions with temperature. 1 wt% CNF suspensions were used for the temperature studies because the viscosity showed the most sensitivity to temperature changes. The rheology of the cellulose nanofiber suspensions was controlled by the temperature of the suspension. For 1 wt% CNF suspensions, the viscosity and shear stress decreased with increasing temperature (Fig. 6).

Temperature dependence was observed in all portions of the strain rate curves, but the change in viscosity and shear stress became more pronounced as the strain rate increased. There is notable separation between each temperature curve in Fig. 6 and there appears to be a more significant change in the rheological properties at lower temperatures, as the distance between the 20 and 25 °C curves is lesser than the difference between the 5 and 10 °C curves.

The temperature dependence of the viscosity of the 1 wt% cellulose suspension was compared to that of pure water at a strain rate of 1 s^{-1} (Table 4). While there was clear decrease in viscosity with increasing temperature in pure water as well as the 1 wt% CNF suspension, the viscosity of the 1 wt% CNF suspension experienced a much more significant change with temperature than the pure water without CNFs. The viscosity of the 1 wt% CNF suspension dropped roughly 30% from 2 °C to 25 °C, while the viscosity of pure water only decreased by roughly 3%.

The shear thinning behavior of the 1 wt% cellulose suspension was also affected by the temperature of the suspension. Using the power law fit of the viscosity (Eq. 1), the shear thinning exponent was calculated and showed a slight increase with temperature, as seen in Table 4. This change in shear thinning exponent was less pronounced than the changes observed by varying cellulose concentration, and the shear thinning behavior was almost independent of temperature.

By fitting the shear stress curves from the strain rate sweep of the 1 wt% CNF suspensions (Fig. 6b) using the Herschel-Bulkley equation (Eq. 2), the yield stress of the suspensions was compared at different temperatures (Table 4). Similar to the trend of the overall shear stress decreasing with increasing temperature, as seen in Fig. 5, the yield stress also decreased as the temperature increased. This is consistent with greater molecular motion at higher temperatures.

Oscillatory frequency sweeps were also conducted to measure the gel-like behavior of 1 wt% CNF suspensions at temperatures below 25 °C. The storage modulus of the suspensions was found to increase as temperature decreased, following the same behavior as the viscosity and yield stress (Fig. 7a). The storage

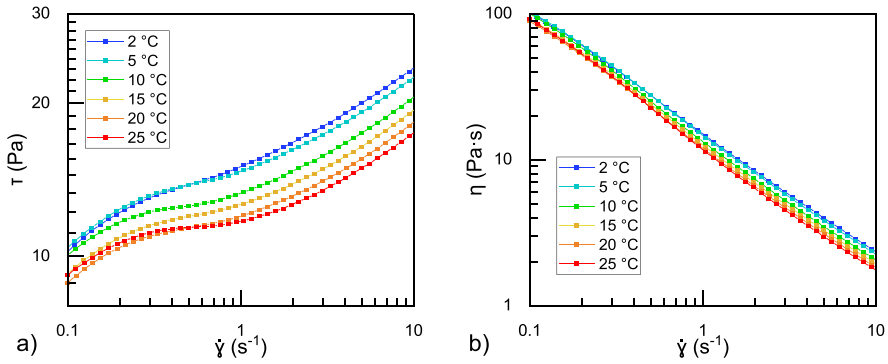

Fig. 6 Viscosity and shear stress of 1 wt% CNF suspensions at varying temperatures. Both the viscosity (**a**) and the shear stress (**b**) increased as the temperature decreased. These plots are representative of the trend seen across 3–5 replicates for each temperature

Table 4 Viscosity, shear thinning behavior, and yield stress of 1 wt% CNF with temperature

Temperature (°C)	Viscosity of pure water* (Pa·s)	Viscosity of 1 wt% CNF* (Pa·s)	Shear Thinning Exponent of 1 wt% CNF	Yield Stress of 1 wt% CNF (Pa)
2		14.4 +/- 0.1	0.84 +/- 0.01	11.5 +/- 0.8
5	0.0838 +/- 0.0005	13.4 +/- 0.6	0.85 +/- 0.01	11.0 +/- 0.4
10	0.0825 +/- 0.0003	12.7 +/- 0.1	0.86 +/- 0.01	10.6 +/- 0.2
15	0.0820 +/- 0.0003	12.3 +/- 0.1	0.86 +/- 0.01	10.5 +/- 0.1
20	0.0819 +/- 0.0001	11.3 +/- 0.3	0.87 +/- 0.01	9.8 +/- 0.2
25	0.0813 +/- 0.0006	10.3 +/- 0.9	0.89 +/- 0.01	8.9 +/- 1

* The viscosity of the suspensions was measured at a strain rate of 1 s^{-1}.

modulus measured at 1 Hz revealed a power law relationship between temperature and storage modulus of the 1 wt% cellulose suspension (Fig. 7b).

In the temperature range of 2 °C to 25 °C, the rheology of cellulose suspensions was found to be highly dependent on the temperature. The viscosity, yield stress, and storage and loss moduli were all found to decrease as the temperature increased, while the shear thinning exponent showed a slight increase with temperature.

Discussion

Strain rate sweeps

The viscosity of the CNF suspensions increased with the concentration of CNFs as there were more fibers to form entanglements between themselves to resist the flow. The 0.1 wt% CNF suspension did not have a sufficient concentration of nanofibers to form a network, so the fibers could not entangle to give structure to the suspension, and therefore it behaved similar to pure water when shear was applied. The shear stress of the cellulose suspensions increased with shear rate as the bundles of cellulose nanofibers were brought into contact and began entangling. Shear stress and yield stress increased with cellulose concentration as there was a higher concentration of fibril bundles to form entanglements, increasing the strength and resistance to flow of the material. This is in good agreement with literature, as many sources report the increase in shear stress and viscosity with cellulose concentration (Pääkkö et al. 2007; Li et al. 2015; Naderi 2017; Wu et al. 2014). Similarly, the yield stress calculated from the Herschel-Bulkley equation demonstrates an increase with cellulose concentration consistent with literature, although

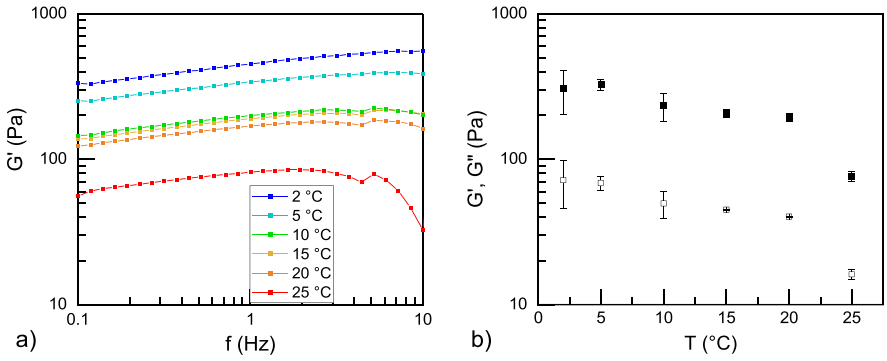

Fig. 7 Storage modulus from oscillatory frequency sweeps of 1 wt% CNF suspensions at various temperatures (**a**) and the temperature dependence of storage (filled symbols) and loss (open symbols) moduli at a frequency of 1 Hz (**b**). Both the storage and loss moduli decreased as the temperature increased. These plots are representative of the trends seen in 3–5 replicates for each temperature

different testing conditions were used (O'Banion and Shams Es-haghi 2023).

As the shear rate increased the attractive interactions between the cellulose molecules and the water molecules were deformed because of the high kinetic energy applied. Three different regions were identified based on the applied shear rate, 0.01 to 0.1 s^{-1}, 0.1 to 10 s^{-1}, and 10 and 100 s^{-1}, which is consistent with what has been observed in literature (Li et al. 2015; Iotti et al. 2011; Nechyporchuk et al. 2016). At low shear rates (below 0.1 s^{-1}), the viscosity was almost constant with shear rate, and did not yet display shear thinning behavior. This was due to both systematic error (surface tension effects, low torque, and data integration time) and because the CNF suspensions initially resisted flow before they began to assemble into chain-like structures and form flocs. At intermediate shear rates, from 0.1 to 10 s^{-1}, the CNF suspensions demonstrated clear shear thinning behavior with a power law relationship between viscosity and shear rate. At high shear rates, between 10 and 100 s^{-1}, the fibers continued entangling and forming flocs until a critical strain was reached where the flocs became unstable and irreversibly aggregated. As the pure water sample also demonstrated an increase in viscosity at high strain rates, the high rotational speed likely contributed to erroneous measurements of viscosity and shear stress in this regime, exaggerating the effects of entanglements in the CNF solutions.

The shear thinning properties of cellulose suspensions arise from the balance of entanglements between the cellulose fibrils and the increasing shear rate. Initially, as shear rate increases, more cellulose fibers are brought into contact with each other, entangling and increasing viscosity. At the same time, the higher shear rate disrupts the entangled structures, aligning them with the flow direction and breaking them down into smaller bundles, decreasing the viscosity. At higher shear rates, shear thinning behavior arises from increased breakdown of the cellulose entanglements. As a result, at higher concentrations of cellulose this effect becomes more pronounced, resulting in a much larger difference in the viscosity at high and low shear rates and therefore a higher shear thinning exponent (Table 2). The increase of a shear thinning exponent with cellulose concentration has been reported by Quennouz et al., who noted an increase from $n=0.37$ at 0.3 wt% CNFs to $n=0.86$ at 1.2% CNFs (Quennouz, 2016). Although they were using a different source of CNFs, and tested different concentrations at a different temperature, their data supports the trend observed in this work. This behavior can be beneficial for applications using higher concentrations of cellulose, where the higher viscosity of the suspension would usually hinder the flow of the material. Although the increased viscosity results in greater resistance to initial flow, as the material begins shearing, the enhanced shear thinning behavior leads to easier movement of the material over time, while still maintaining the benefits of a higher viscosity suspension overall. Cellulose is also thixotropic (Jiang et al. 2021; Iotti et al. 2011; O'Banion and Shams Es-haghi 2023), which means the flow behavior changes over time regardless of shear, further improving the flow properties of cellulose suspensions over time.

Oscillatory sweeps

The oscillatory strain sweeps confirmed the storage and loss moduli of the cellulose suspensions were all constant in the linear viscoelastic range, which went until roughly 0.001 strain at 1 wt% CNFs, and closer to a strain of 0.01 for the 0.5 wt% CNFs. At higher strains the gel-like structure formed by the suspension begins to change and breakdown from the high strain, resulting in a decrease in the storage moduli. The oscillatory strain sweep showed that the 0.5 and 1 wt% cellulose suspensions were yield stress fluids that have a static yield strength that needs to be reached before the material will flow. The 0.5 wt% and 1 wt% CNF suspensions formed a stronger gel network and displayed more solid-like behavior, with a higher storage modulus than loss modulus, while the 0.1 wt% CNF suspension behaved more liquid-like, with a higher loss modulus than storage modulus, and did not show any gel-like characteristics. Observing the storage and loss moduli with an oscillatory frequency sweep in the LVR revealed that for all CNF suspensions the moduli appear to be almost frequency independent, with a slight dependence on applied frequency. There was a clear increase in storage moduli with cellulose concentration, as the higher number of entanglements increased in the more concentrated suspensions to form a stronger gel-like structure. The trend in the increase in storage modulus with cellulose concentration clearly matches the power law relationship observed in literature (Nechyporchuk et al. 2016).

An oscillatory stress sweep was used as a secondary method for yield stress analysis of the cellulose suspensions. Oscillatory stress sweeps are typically used for yield analysis of higher viscosity materials that do not reveal yield stresses in dynamic strain rate measurements. Although a Herschel-Bulkley fit was applied to the dynamic strain rate tests to determine the yield stress of the cellulose suspensions, the yield stress was not immediately obvious in the continuous flow experiments without fitting the data. In the oscillatory test the CNF suspensions clearly demonstrated behavior indicative of yield stress fluids with a change in slope of both strain and storage moduli at a critical applied stress value. This critical stress was the yield stress, which increased with cellulose concentration and therefore showed that higher concentrations of cellulose show stronger gel-like behavior. In structured fluids, the higher the storage modulus and yield stress, the stronger the material resistance is to sedimentation and structural breakdown. This is extremely important for using CNF suspensions for polymer gels, aerogels, and structural applications to ensure the cellulose fibral network stays intact while the composite material sets, cures, or evaporates.

Temperature dependence

The viscosity, moduli, shear stress, and shear thinning behavior of 1 wt% CNF suspensions were all dependent on the CNF suspension temperature, ranging from 2 °C to 25 °C. As the temperature of the suspension decreases, the molecules in the suspension have less thermal energy and the distance between the molecules is reduced, so the intermolecular forces are stronger. The higher intermolecular forces result in more resistance to flowing the material, which is represented by a higher viscosity. For this same reason, the shear stresses experienced by the CNF suspensions increased as the temperature decreased, which is reflected in the yield stress calculations. The increased intermolecular forces result in a higher torque needed to shear the material at the same rate, resulting in a higher stress experienced in the material. Although it is well known that the viscosity of water increases with decreasing temperature, the changes in viscosity of the 1 wt% CNF suspensions were much more significant than what was observed in pure water, implying that the viscosity dependence on temperature is more strongly related to the interactions between the cellulose molecules, not the water they are suspended in.

Despite the increase in the viscosity of the CNF suspensions at lower temperature, the shear thinning behavior of the suspensions showed the opposite trend, as the shear thinning constant increased with increasing temperature. At higher temperatures shear thinning effects are more pronounced as the higher energy in the suspension more readily disrupts the interactions between the molecules in the suspension. As the temperature decreases, the kinetic energy in the suspension decreases, so as the shear rate increases there is insufficient kinetic energy to overcome the entanglements of the cellulose fibers.

The storage modulus was also dependent on temperature, with the moduli increasing with decreasing temperature, indicating that a stronger gel-like network forms at lower temperatures. Interestingly, one literature report on the rheology of 1–6 wt% MFC (microfibrillated cellulose) in the temperature range of 20–80 °C found that the moduli increased as temperature increased (Pääkkö et al. 2007). Another publication reported a constant moduli over the temperature range of 25–60 °C for 3 wt% CMF (cellulose microfibrils) (Lowys et al. 2001). Pääkkö et al. and Lowys et al. each describe different trends than we report herein; however, our temperature range (2 to 25 °C) does not overlap with the ranges they examined (20–80 °C and 25–60 °C respectively) so a robust trend for the modulus of cellulose over a broad temperature range is not yet available.

Similar to the storage modulus results, our viscosity results showed an inverse correlation to temperature, increasing with decreasing temperature. Nechyporchuk et al. discussed that the storage modulus behaved opposite to viscosity in cellulose as a function of temperature because gels behave differently in the linear viscoelastic region versus under flow (rotational measurements). Because we did not observe the same trend, we can surmise that our CNF suspensions behave similarly under oscillatory and rotational action over the temperature range of 2 to 25 °C (Nechyporchuk et al. 2016). There are multiple reasons why we may have observed different trends than have previously been reported. Both sources use micro fibrillated cellulose suspensions, rather than nanocellulose, and use a higher concentration of fibers, which change the intermolecular interactions (e.g., entanglement) present in the suspension.

Additionally, we used a different geometry for our testing. Rather than the cone and plate geometry, we used a cup and rotor for oscillatory measurements because we had lower viscosity suspensions. Although we used a serrated cup, this would still result in wall interactions that are not present in the cone and plate geometry. Existing literature reports on the rheology of cellulose suspensions were all conducted at or above room temperature, and there is a lack of reports on cellulose dispersions as they approach the thermodynamic freezing point of water. It is possible that as the CNF suspensions are cooled below room temperature, their rheological behavior is governed by different mechanisms than at higher temperatures.

Conclusions

Overall, the viscosity, shear stress, shear thinning, and storage modulus were all found to be dependent on cellulose concentration and suspension temperature. These differences were observed using both steady flow rotational measurements as well as oscillatory measurements in the linear viscoelastic range. Our data matches trends seen in literature confirming the shear thinning behavior of cellulose. This behavior was enhanced with increasing cellulose concentration and at lower temperatures. Similarly, the apparent viscosity, shear stress, and storage modulus were confirmed to all increase with increasing cellulose concentration and decreasing temperature. The 0.5 and 1 wt% CNF mixtures formed gel-like suspensions and were shown to be yield stress fluids. However, the 0.1 wt% CNF suspension did not form a gel because the concentration was below the critical concentration needed to form an entangled network. The temperature dependence of the 1 wt% CNF suspensions was heightened compared to pure water, indicating the changes in viscosity and strength as a function of temperature were related to changes in the polymer chains interactions.

The rheological properties of cellulose suspensions demonstrate good behavior as an additive for polymer extrusions, gels, or other applications that aim to use the high strength of cellulose fibers. The shear thinning behavior of cellulose suspensions allows for easier flow of the material, while the yield strength is sufficient to provide support for polymer scaffolds or composites. The properties of these CNF suspensions can be tuned by modifying the temperature of the suspension to achieve the desired viscosity or strength. This is promising for applications using lower temperature material processing methods, such as ice templating, or suspensions exposed to colder environments.

Acknowledgements The authors are grateful to Matthew Fort for support during experimental setup and to Eftihia Barnes for AFM characterization of the CNFs.

Author contributions All authors contributed to the study conception and design. Material preparation, data collection, and analysis were performed by KTT. The first draft of the manuscript was written by KTT and all authors contributed content to revisions of the manuscript. All authors have read and approved the final manuscript.

Funding US Army Engineer Research and Development Center, Installations and Operational Environments Basic Research Program (A1050-T23/T177).

Data availability No datasets were generated or analysed during the current study.

Declarations

Competing interests The authors declare no competing interests.

References

Ardanuy M, Claramunt J, Toledo Filho RD (2015) Cellulosic fiber reinforced cement-based composites: a review of recent research. Constr Build Mater 79:115–128. https://doi.org/10.1016/j.conbuildmat.2015.01.035

Baniasadi H, Kimiaei E, Polez RT, Ajdary R, Rojas OJ, Österberg M, Seppälä J (2022) High-resolution 3D printing of xanthan gum/nanocellulose bio-inks. Int J Biol Macromol 209:2020–2031. https://doi.org/10.1016/j.ijbiomac.2022.04.183

Bledzki AK, Gassan J (1999) Composites reinforced with cellulose based fibres. Prog Polym Sci 24(2):221–274. https://doi.org/10.1016/S0079-6700(98)00018-5

Das R, Lindström T, Sharma PR, Chi K, Hsiao BS (2022) Nanocellulose for Sustainable Water Purification. Chem Rev 122(9):8936–9031. https://doi.org/10.1021/acs.chemrev.1c00683

Erlandsson J, Pettersson T, Ingverud T, Granberg H, Larsson PA, Malkoch M, Wågberg L (2018) On the mechanism behind freezing-induced chemical crosslinking in ice-templated cellulose nanofibril aerogels. J Mater Chem A 6(40):19371–19380. https://doi.org/10.1039/c8ta06319b

Fall AB, Lindström SB, Sundman O, Ödberg L, Wågberg L (2011) Colloidal Stability of Aqueous Nanofibrillated Cellulose Dispersions. Langmuir 27(18):11332–11338. https://doi.org/10.1021/la201947x

Flauder S, Heinze T, Müller FA (2013) Cellulose scaffolds with an aligned and open porosity fabricated via ice-templating. Cellulose 21(1):97–103. https://doi.org/10.1007/s10570-013-0119-9

Flory PJ (1974) Introductory lecture. Faraday Discuss Chem Soc 57(0):7–18. https://doi.org/10.1039/DC9745700007

Geng L, Mittal N, Zhan C, Ansari F, Sharma PR, Peng X, Hsiao BS, Söderberg LD (2018) Understanding the mechanistic behavior of highly charged cellulose nanofibers in Aqueous systems. Macromolecules 51(4):1498–1506. https://doi.org/10.1021/acs.macromol.7b02642

Guan QF, Yang HB, Han ZM, Zhou LC, Zhu YB, Ling ZC, Jiang HB, Wang PF, Ma T, Wu HA, Yu SH (2020) Lightweight, tough, and sustainable cellulose nanofiber-derived bulk structural materials with low thermal expansion coefficient. Sci Adv 6(18):8. https://doi.org/10.1126/sciadv.aaz1114

Gupta S, Martoïa F, Orgéas L, Dumont P (2018) Ice-templated porous nanocellulose-based materials: current Progress and opportunities for materials Engineering. Appl Sci 8(12). https://doi.org/10.3390/app8122463

Habibi Y, Lucia LA, Rojas OJ (2010) Cellulose nanocrystals: Chemistry, Self-Assembly, and applications. Chem Rev 110(6):3479–3500. https://doi.org/10.1021/cr900339w

Hausmann MK, Rühs PA, Siqueira G, Läuger J, Libanori R, Zimmermann T, Studart AR (2018) Dynamics of Cellulose Nanocrystal Alignment during 3D Printing. ACS Nano 12(7):6926–6937. https://doi.org/10.1021/acsnano.8b02366

Heggset EB, Strand BL, Sundby KW, Simon S, Chinga-Carrasco G, Syverud K (2019) Viscoelastic properties of nanocellulose based inks for 3D printing and mechanical properties of CNF/alginate biocomposite gels. Cellulose 26(1):581–595. https://doi.org/10.1007/s10570-018-2142-3

Herrick FW, Casebier RL, Hamilton JK, Sandberg KR (1983) Microfibrillated cellulose: morphology and accessibility. Journal Name: J. Appl. Polym. Sci.: Appl. Polym. Symp.; (United States); Journal Volume: 37; Conference: 9. cellulose conference, Syracuse, NY, USA, 24 May 1982, United States

Hubbe MA, Rojas OJ, Lucia LA, Sain MM (2008) CELLULOSIC NANOCOMPOSITES: A REVIEW. BioResources 3:929–980

Huber T, Müssig J, Curnow O, Pang S, Bickerton S, Staiger MP (2012) A critical review of all-cellulose composites. J Mater Sci 47(3):1171–1186. https://doi.org/10.1007/s10853-011-5774-3

Iotti M, Gregersen ØW, Moe S, Lenes M (2011) Rheological Studies of Microfibrillar Cellulose Water Dispersions. J Polym Environ 19(1):137–145. https://doi.org/10.1007/s10924-010-0248-2

Jiang J, Oguzlu H, Jiang F (2021) 3D printing of lightweight, super-strong yet flexible all-cellulose structure. Chem Eng J 405:126668. https://doi.org/10.1016/j.cej.2020.126668

Karppinen A, Saarinen T, Salmela J, Laukkanen A, Nuopponen M, Seppälä J (2012) Flocculation of microfibrillated cellulose in shear flow. Cellulose 19(6):1807–1819. https://doi.org/10.1007/s10570-012-9766-5

Koponen AI (2020) The effect of consistency on the shear rheology of aqueous suspensions of cellulose micro- and nanofibrils: a review. Cellulose 27(4):1879–1897. https://doi.org/10.1007/s10570-019-02908-w

Li M-C, Wu Q, Song K, Lee S, Qing Y, Wu Y (2015) Cellulose nanoparticles: structure–morphology–Rheology relationships. ACS Sustain Chem Eng 3(5):821–832. https://doi.org/10.1021/acssuschemeng.5b00144

Li T, Chen C, Brozena AH, Zhu JY, Xu L, Driemeier C, Dai J, Rojas OJ, Isogai A, Wågberg L, Hu L (2021) Developing fibrillated cellulose as a sustainable technological material. Nature 590(7844):47–56. https://doi.org/10.1038/s41586-020-03167-7

Liu H, Du H, Zheng T, Liu K, Ji X, Xu T, Zhang X, Si C (2021) Cellulose based composite foams and aerogels for advanced energy storage devices. Chem Eng J 426:130817. https://doi.org/10.1016/j.cej.2021.130817

Lowys MP, Desbrières J, Rinaudo M (2001) Rheological characterization of cellulosic microfibril suspensions. Role of polymeric additives. Food Hydrocolloids 15(1):25–32. https://doi.org/10.1016/S0268-005X(00)00046-1

Malkin AY, Derkach SR, Kulichikhin VG (2023) Rheology of gels and yielding liquids. Gels 9(9):715

Martoïa F, Cochereau T, Dumont PJJ, Orgéas L, Terrien M, Belgacem MN (2016) Cellulose nanofibril foams: links between ice-templating conditions, microstructures and mechanical properties. Mater Design 104:376–391. https://doi.org/10.1016/j.matdes.2016.04.088

Naderi A (2017) Nanofibrillated cellulose: properties reinvestigated. Cellulose 24(5):1933–1945. https://doi.org/10.1007/s10570-017-1258-1

Nanocellulose Data Sheets The University of Maine. https://umaine.edu/pdc/nanocellulose/nanocellulose-spec-sheets-and-safety-data-sheets/

Navard P, Wendler F, Meister F, Bercea M, Budtova T (2012) Preparation and properties of Cellulose solutions. The European Polysaccharide Network of Excellence (EPNOE): Research Initiatives and results. Vienna, pp 91–152

Nechyporchuk O, Belgacem MN, Pignon F (2015) Concentration effect of TEMPO-oxidized nanofibrillated cellulose aqueous suspensions on the flow instabilities and small-angle X-ray scattering structural characterization. Cellulose 22(4):2197–2210. https://doi.org/10.1007/s10570-015-0640-0

Nechyporchuk O, Belgacem M, Pignon F (2016) Current progress in Rheology of Cellulose Nanofibril suspensions. Biomacromolecules 17 7:2311–2320

O'Banion EE, Es-haghi S S (2023) Rheological behavior of cellulose nanofibril suspensions with varied levels of fines and solid content. Polymer 288:126445. https://doi.org/10.1016/j.polymer.2023.126445

Pääkkö M, Ankerfors M, Kosonen H, Nykänen A, Ahola S, Österberg M, Ruokolainen J, Laine J, Larsson PT, Ikkala O, Lindström T (2007) Enzymatic hydrolysis combined with mechanical shearing and high-pressure homogenization for Nanoscale cellulose fibrils and strong gels. Biomacromolecules 8(6):1934–1941. https://doi.org/10.1021/bm061215p

PDC Services The University of Maine. https://umaine.edu/pdc/facilities-available-for-use/

Quennouz N, Hashmi SM, Choi HS, Kim JW, Osuji CO (2016) Rheology of cellulose nanofibrils in the presence of surfactants. Soft Matter 12(1):157–164

Seddiqi H, Oliaei E, Honarkar H, Jin J, Geonzon LC, Bacabac RG, Klein-Nulend J (2021) Cellulose and its derivatives: towards biomedical applications. Cellulose 28(4):1893–1931. https://doi.org/10.1007/s10570-020-03674-w

Sen S, Singh A, Bera C, Roy S, Kailasam K (2022) Recent developments in biomass derived cellulose aerogel materials for thermal insulation application: a review. Cellulose 29(9):4805–4833. https://doi.org/10.1007/s10570-022-04586-7

Sharma A, Thakur M, Bhattacharya M, Mandal T, Goswami S (2019) Commercial application of cellulose nano-composites – a review. Biotechnol Rep 21:e00316. https://doi.org/10.1016/j.btre.2019.e00316

Shi Z, Zhang Y, Phillips GO, Yang G (2014) Utilization of bacterial cellulose in food. Food Hydrocolloids 35:539–545. https://doi.org/10.1016/j.foodhyd.2013.07.012

Velásquez-Cock J, Serpa A, Vélez L, Gañán P, Gómez Hoyos C, Castro C, Duizer L, Goff HD, Zuluaga R (2019) Influence of cellulose nanofibrils on the structural elements of ice cream. Food Hydrocolloids 87:204–213. https://doi.org/10.1016/j.foodhyd.2018.07.035

Wu Q, Meng Y, Wang S, Li Y, Fu S, Ma L, Harper D (2014) Rheological behavior of cellulose nanocrystal suspension: influence of concentration and aspect ratio. J Appl Polym Sci 131(15). https://doi.org/10.1002/app.40525

Yasim-Anuar TAT, Ariffin H, Norrrahim MNF, Hassan MA, Andou Y, Tsukegi T, Nishida H (2020) Well-dispersed cellulose Nanofiber in Low Density Polyethylene Nanocomposite by Liquid-assisted extrusion. Polym (Basel) 12(4). https://doi.org/10.3390/polym12040927

Zambrano F, Starkey H, Wang Y, Assis CA, d, Venditti RA, Pal L, Jameel H, Hubbe MA, Rojas OJ, Gonzalez R (2020) Using micro- and nanofibrillated cellulose as a means to reduce weight of paper products: a review. BioResources

Zhu M, Huan S, Liu S, Li Z, He M, Yang G, Liu S, McClements DJ, Rojas OJ, Bai L (2021) Recent development in food emulsion stabilized by plant-based cellulose nanoparticles. Curr Opin Colloid Interface Sci 56:101512. https://doi.org/10.1016/j.cocis.2021.101512